Acta Crystallographica Section C
Crystal Structure Communications
ISSN 0108-2701

Methyl β-allolactoside [methyl β-D-galactopyranosyl-(1→6)-β-D-glucopyranoside] monohydrate

Thomas E. Klepach,[a] Meredith Reed,[b] Bruce C. Noll,[a] Allen G. Oliver[a] and Anthony S. Serianni[a]*

[a]Department of Chemistry and Biochemistry, 251 Nieuwland Science Hall, University of Notre Dame, Notre Dame, IN 46556-5670, USA, and [b]Omicron Biochemicals Inc., South Bend, IN 46617, USA
Correspondence e-mail: anthony.s.serianni.1@nd.edu

Received 8 September 2009
Accepted 15 October 2009
Online 7 November 2009

Methyl β-allolactoside [methyl β-D-galactopyranosyl-(1→6)-β-D-glucopyranoside], (II), was crystallized from water as a monohydrate, $C_{13}H_{24}O_{11}\cdot H_2O$. The βGal*p* and βGlc*p* residues in (II) assume distorted $^4C_1$ chair conformations, with the former more distorted than the latter. Linkage conformation is characterized by φ' ($C2_{Gal}-C1_{Gal}-O1_{Gal}-C6_{Glc}$), ψ' ($C1_{Gal}-O1_{Gal}-C6_{Glc}-C5_{Glc}$) and ω ($C4_{Glc}-C5_{Glc}-C6_{Glc}-O1_{Gal}$) torsion angles of 172.9 (2), −117.9 (3) and −176.2 (2)°, respectively. The ψ' and ω values differ significantly from those found in the crystal structure of β-gentiobiose, (III) [Rohrer *et al.* (1980). *Acta Cryst.* B**36**, 650–654]. Structural comparisons of (II) with related disaccharides bound to a mutant β-galactosidase reveal significant differences in hydroxymethyl conformation and in the degree of ring distortion of the βGlc*p* residue. Structural comparisons of (II) with a DFT-optimized structure, (II_C), suggest a link between hydrogen bonding, pyranosyl ring deformation and linkage conformation.

Comment

The disaccharide β-D-galactopyranosyl-(1→6)-D-glucopyranose (allolactose), (I), is widely known as an inducer of the *lac* operon. Allolactose serves as a negative allosteric effector of the *lac* repressor (LacI) (Jacob & Monod, 1961; Burstein *et al.*, 1965; Jobe & Bourgeois, 1972; Yildirim & Mackey, 2003). In *E. coli*, lactose [β-D-galactopyranosyl-(1→4)-D-glucopyranose] is converted to (I) *via* transglycosylation catalyzed by β-galactosidase (Jacob & Monod, 1961; Burstein *et al.*, 1965; Jobe & Bourgeois, 1972). The crystal structure of (I) has not been reported, but it appears in 1.5 Å resolution cocrystals with a mutant β-galactosidase (Juers *et al.*, 2001). In addition to its biological role as a free disaccharide, the β-D-Gal*p*-(1→6)-β-D-Glc*p* glycosidic linkage is observed in various glycoconjugates, including a ceramide trisaccharide, β-D-Gal*p*(1→6)-β-D-Gal*p*-(1→6)-β-D-Glc*p*-(1→1)-Cer, isolated from sea urchin eggs (Kubo *et al.*, 1992), and in the soluble protein bovine lactoferrin (Mir *et al.*, 2009).

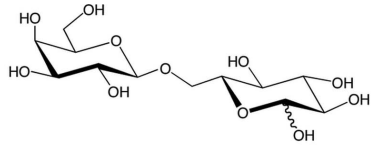

β-D-galactopyranosyl-(1→6)-α/β-D-glucopyranose
allolactose (I)

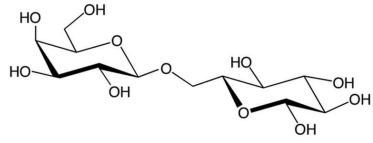

β-D-galactopyranosyl-(1→6)-β-D-glucopyranose
β-allolactose (I_β)

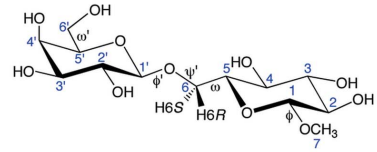

methyl β-D-galactopyranosyl-(1→6)-β-D-glucopyranoside
methyl β-allolactoside (II)

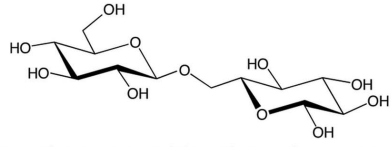

β-D-glucopyranosyl-(1→6)-β-D-glucopyranose
β-gentiobiose (III)

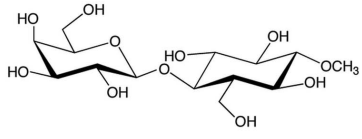

methyl β-D-galactopyranosyl-(1→4)-β-D-glucopyranoside
methyl β-lactoside (IV)

As structural information on the β-Gal-(1→6)-β-Glc linkage in differing biological contexts grows, the geometry of the isolated disaccharide, to which comparisons with more complex structures can be made, increases in importance. We report here the crystal structure of the methyl glycoside of (I), namely methyl β-D-galactopyranosyl-(1→6)-β-D-glucopyranoside (methyl β-allolactoside) monohydrate, $(II)\cdot H_2O$ (Fig. 1). Atom numbering is shown in the structure of (II), with primed and unprimed numbers assigned to the βGal*p* and βGlc*p* residue atoms, respectively. Structural parameters found for (II) were compared with those observed in β-gentiobiose [β-D-glucopyranosyl-(1→6)-β-D-glucopyranose], (III) (Arène *et al.*, 1979; Rohrer *et al.*, 1980), which is the only structurally related (1→6)-linked disaccharide whose crystal structure is known. Comparisons were also made with structures of (I_β) bound to β-galactosidase (Juers *et al.*, 2001), denoted (I_{G1}), (I_{G2}) and

 doi:10.1107/S0108270109042310

(I_{G3}), and with methyl β-D-galactopyranosyl-(1→4)-β-D-glucopyranoside (methyl β-lactoside), (IV) (Stenutz *et al.*, 1999) (Table 1). The influence of crystal packing on structural parameters was also investigated in an unconstrained *in vacuo* density functional theory (DFT) geometry optimization using *GAUSSIAN03* (Frisch *et al.*, 2004). The crystal structure of (II) was used as the starting geometry and the calculation was performed with the B3LYP functional (Becke, 1993), and the 6–31G* basis set (Hehre *et al.*, 1972). Structural data for the DFT structure, denoted (II_C), are shown in Table 1.

Data in Table 1 for (II)–(IV) yield the following average C—C bond lengths: C1—C2 = 1.522 (6) Å; remaining endocyclic C—C = 1.526 (7) Å; C5—C6 = 1.511 (3) Å. Exocyclic C5—C6 bonds appear shorter than all endocyclic C—C bonds (Pan *et al.*, 2005), while C1—C2 bond lengths do not differ statistically from the other endocyclic C—C bond lengths.

Average C—O bond lengths in (II)–(IV) are as follows: endocyclic C—O = 1.425 (9) Å; anomeric C—O (exocyclic) = 1.392 (6) Å; exocyclic C—O = 1.426 (8) Å; exocyclic C—O involving the anomeric oxygen = 1.434 (8) Å. The equatorial C1—O1 and C1′—O1′ bonds are shorter (by ∼0.03 Å) than the remaining exocyclic equatorial C—O bonds (Berman *et al.*, 1967), due to optimal anomeric effects (Lemieux, 1971) in these structures; in (II), the C2′—C1′—O1′—C6 and C2—C1—O1—C7 torsion angles are 172.9 (2) and 177.4 (3)°, respectively.

In the DFT-calculated structure (II_C), trends in C—C bond lengths mimic the experimental observations, but calculated C—C bond lengths are longer on average than experimental values by ∼0.01 Å: C1—C2 = 1.531 (3) Å; remaining endocyclic C—C = 1.532 (8) Å; C5—C6 = 1.525 (3) Å. In contrast, DFT-calculated C—O bond lengths reproduce the experimental data well, both in terms of trends and absolute values: endocyclic C—O = 1.426 (6) Å; anomeric C—O (exocyclic) = 1.393 (6) Å; exocyclic C—O = 1.421 (6) Å; exocyclic C—O involving the anomeric oxygen = 1.430 Å.

The C4′—O4′ bond lengths in (II) and (III) are identical despite differences in C4 configuration (Table 1). The C4′—O4′ bond conformation in (II) and (III) cannot be responsible for this finding, since both bonds are in conformations in which the C4′ and O4′ H atoms are eclipsed. Intermolecular hydrogen bonding in the C4′—O4′ fragment of both (II) and (III) is also identical. In contrast, $r_{C4',O4'}$ is considerably shorter in (II_C) than in (II) and (III), presumably due, at least partly, to relief of the eclipsing interaction in the calculated structure [the equivalent C4′ and O4′ H atoms are approximately *gauche* in (II_C)]. These findings suggest that the relative lengths of axial and equatorial C—O bonds in saccharides can be influenced significantly by crystal packing forces, and that eclipsing interactions present in crystal structures caused by the intermolecular hydrogen-bonding lattice may suppress competing intramolecular forces that affect exocyclic C—O bond lengths (*e.g.* bond orientation). The internal glycosidic C—O—C bond angle in (II) and (III) appears slightly smaller than observed in (IV), possibly due to the reduced steric demands of the 1,6-linkage. This conclusion is supported by glycosidic C—O—C bond angles involving the methyl aglycones in (II) and (III), which compare favorably to the internal glycoside C—O—C angles in the same structures.

The β-Glc*p* and β-Gal*p* rings of (II)–(IV) assume slightly distorted $^4C_1$ chair conformations based on Cremer–Pople puckering parameters (Cremer & Pople, 1975; Table 2; $q_3 >> q_2$). In (II), the β-Glc*p* ring is closer to an ideal $^4C_1$ chair form (θ = 2.3°) than the β-Gal*p* ring (θ = 8.8°), whereas the opposite is found for (IV). In (III), both rings have more comparable θ values and thus comparable degrees of distortion. The direction of distortion, embodied in φ, is context dependent and can be easily visualized using the projection convention of Jeffrey & Yates (1979) (Fig. 2). Overall, global ring shapes for the β-Gal*p* ring of (IV) and the β-Glc*p* rings of (III) [φ = 28 (6)°] are slightly distorted near $^0H_1$; these conformations differ from the β-Gal*p* ring of (II) and the β-Glc*p* rings of (II) and (IV) which are distorted near E_5 and $^0E/^0H_5$, respectively.

Exocyclic hydroxymethyl (–CH_2OH) conformations in (II)–(IV), denoted by torsion angle ω, differ. In (II), the *gt* (*gauche–trans*) conformation is found in both residues, whereas in (III), *gg* (*gauche–gauche*) conformations are observed (Table 1), resulting in significantly different surface topologies for the two disaccharides. In contrast, mixed conformations are found in (IV), *viz.* *gg* in β-Glc*p* and *gt* in β-Gal*p*. The *gt* conformation is highly favored in methyl β-D-galactopyranoside in aqueous solution, based on NMR scalar coupling analysis, whereas a roughly equal mixture of *gg* and *gt* forms is observed in methyl β-D-glucopyranoside (Thibaudeau *et al.*, 2004), results consistent with the statistical distribution of rotamers observed in (II)–(IV).

Glycosidic linkage conformation in (II) is determined by torsion angles φ' [C2′—C1′—O1′—C6 = 172.9 (2)°], ψ' [C1′—O1′—C6—C5 = −117.9 (3)°] and ω [O1′—C6—C5—O5 = 63.8 (3)°]. These torsions contrast with corresponding values of −176.4, −156.3 and −61.6° observed in (III). The φ' values differ by ∼11°, whereas the ψ' values differ by ∼38°. Presumably, different conformations about ω and ω' in (II) and (III) influence ψ', which is controlled mainly by steric

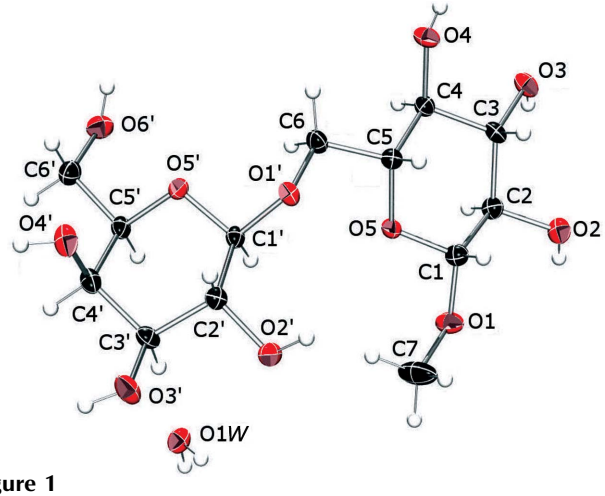

Figure 1
The crystal structure and atom-labeling scheme of (II). Displacement ellipsoids are depicted at the 50% probability level.

factors rather than the stereoelectronic (exoanomeric; Lemieux, 1971) factors that largely influence φ'. It is noteworthy that φ' values in (II)–(III) are larger than the corresponding value in (IV) (153.8°), which suggests reduced steric constraints for the linkage in the former and leading to nearly ideal, *i.e.* perfectly staggered, exoanomeric conformations for both C1′—O1′ bonds.

Linkage conformation in the DFT-calculated structure (II_C) is similar to that in (II); the glycosidic torsion angles φ' and ψ' differ by ∼12° (Table 1). While Cremer–Pople θ values differ by < 2.4°, the types of ring distortions in (II) and (II_C) differ, especially for the βGal*p* ring, where φ values differ by ∼90° (Table 2). The discrepancy may be linked to a change in hydrogen bonding involving the C3′ and C4′ hydroxy groups from the intermolecular arrangement in (II) (see below) to an intramolecular hydrogen bond (O4′···O3′) in (II_C) [$r_{O3',O4'}$ in (II_C) = 2.693 Å]. Ring-puckering amplitudes, Q, decrease by 3.2 and 3.5% for the βGal*p* and βGlc*p* residues, respectively, in (II_C) relative to (II).

Crystal structures of mutant β-galactosidase complexed with (I_β) (Juers *et al.*, 2001) reveal the degree to which the βGal(1→6)βGlc structure is deformed upon protein binding (Table 3). The glycosidic torsions φ' are very similar for (II) and ($I_{G1–G3}$) (C2′—C1′—O1′—C6 torsions of 170.0–174.0°), but ψ' values differ considerably (C1′—O1′—C6—C5 torsions of −117.9 to −168.3°). Cremer–Pople θ values are similar for the βGal*p* residue in the free and protein-bound states (Table 2). However, considerable βGlc*p* ring distortion is observed in the bound state, as indicated by the significantly enhanced θ values (Table 2), and the direction of distortion varies widely in the bound geometries. Equally important, exocyclic hydroxymethyl conformation is affected by binding: bound βGal*p* residues assume the *tg* (*trans–gauche*) conformation, whereas *gg* or *gt* is adopted in the βGlc*p* residues (Table 3). In solution, βGal*p* residues prefer *gt* and *tg* conformations, with *gg* virtually absent (Thibaudeau *et al.*, 2004). The statistical findings for ω' in bound conformations of (I_β) are thus consistent with solution behavior. Similar arguments apply to the βGlc*p* residue.

Ring pucker can exert an important effect on glycosidic linkage conformation; deformation of one or both pyranose rings in a β-(1→6) linkage may allow conformations that are not normally accessible. For example, inspections of ($I_{G1–G3}$) and (III) reveal a qualitative correlation between departure from an ideal $^4C_1$ conformation and linkage conformation (Fig. 2). This connectivity suggests that, in solution, a correlation between pyranose ring-puckering dynamics and linkage reorientation may exist. Related behavior has been observed previously in nucleosides (Foloppe & Nilsson, 2005). While furanosyl rings are commonly viewed as more conformationally flexible than pyranosyl rings (Altona & Sundaralingam, 1972, 1973; French & Finch, 1999), pyranose pseudorotation may become more energetically favorable by extrinsic macromolecular forces. This expectation appears to be borne out in the structures of (I_β) bound to mutant β-galactosidase.

The crystal structure of (II) contains no intramolecular hydrogen bonds. Six of the seven hydroxy groups (O3, O4, O2′, O3′, O4′ and O6′) participate as donors in strong intermolecular hydrogen bonds, while the remaining hydroxy group, O2, has longer contacts and is bifurcated between O2′ and O3′ (Table 4 and Fig. 3). Of the seven exocyclic hydroxy O atoms present in (II), five (O2, O3, O3′, O4′, O6′) participate in intermolecular hydrogen bonding as monoacceptors. Hydroxy atom O2′ accepts hydrogen bonds from two donors; one is a weaker bifurcated hydrogen bond described above

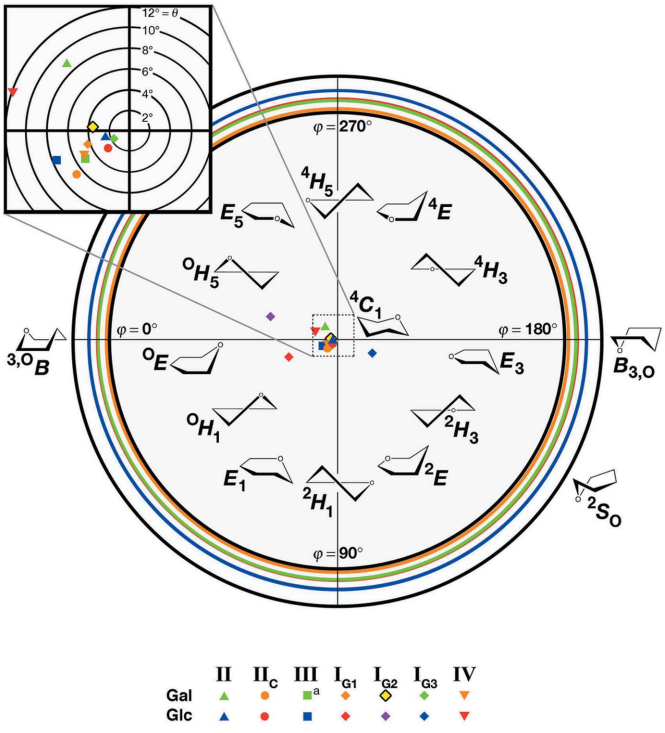

Figure 2
Stereographic projection of the pyranose pseudorotational itinerary (northern hemisphere only) with ring-puckering coordinates for (I)–(IV). Ring-puckering parameters φ and θ are represented by angular and radial displacements about the $^4C_1$ origin (center point), respectively, and displacements are based on individual total puckering amplitudes, Q. In the inset, displacements are based on an average amplitude for the depicted data (Q_{avg} = 0.5734). Inner and outer black rings represent the minimal and maximal Q values for the total data set; colored rings correspond to Q values for the Gal and Glc rings of (II) and (II_C) as per the color code shown below the graphic. The southern hemisphere (not shown) relates *via* symmetry to the northern with $^1C_4$ at the origin. Note: (a) ring at the nonreducing end of (III) is Glc not Gal.

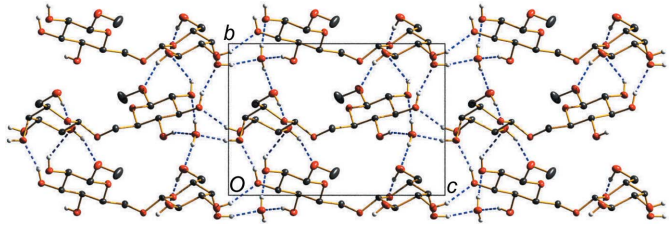

Figure 3
The hydrogen-bonding scheme in the title compound, viewed along the *a* axis.

and the other a more regular hydrogen bond from O6′. The remaining exocyclic hydroxy group, O4, does not receive hydrogen bonds. The two endocyclic O atoms (O5 and O5′) and the internal glycosidic O atom (O1′) are not hydrogen bonded. The remaining terminal glycosidic O atom (O1) serves as a monoacceptor. The water of crystallization (O1*W*) participates as a node, accepting and donating two hydrgoen bonds.

An intermolecular hydrophobic contact in the crystal is observed between the methyl aglycone and the *β*Glc*p* H6*R* and H6*S* hydrogens adjacent to the glycoside from a neighboring unit cell, with methyl–hydroxymethyl H···H internuclear distances of 2.602 and 2.522 Å, respectively. The third methyl H atom has a weaker intramolecular contact with H1′ (3.014 Å).

Experimental

The reagents *o*-nitrophenol, Sepharose G10, Dowex 1 × 2 (200–400 mesh) (Cl^-) ion-exchange resin, *β*-galactosidase (E. C. 3.2.1.23) (*E. coli*) and methyl *β*-D-glucopyranoside were purchased from Sigma.

For the synthesis of *o*-nitrophenyl *β*-D-[1-^{13}C]galactopyranoside, D-[1-^{13}C]galactose was prepared from D-lyxose and K^{13}CN (Cambridge Isotope Laboratories; 99 atom% ^{13}C) by cyanohydrin reduction, yielding D-[1-^{13}C]galactose and D-[1-^{13}C]talose (Serianni *et al.*, 1979, 1990). The *galacto* and *talo* epimers were separated by chromatography on Dowex 50 × 8 (200–400 mesh) (Ca^{2+}) (Angyal *et al.*, 1979), with the *galacto* isomer eluting first. *o*-Nitrophenyl *β*-D-[1-^{13}C]galactopyranoside was prepared from D-[1-^{13}C]galactose in an overall yield of 30% (Conchie & Levvy, 1963).

For the synthesis of (II) by enzyme-catalyzed transglycosylation, the conditions for the transglycosylation reaction were identical to those reported by Nilsson (1987, 1988); the reaction was conducted with 1.35 g (4.48 mmol) of the acceptor (methyl *β*-D-glucopyranoside) and 2.50 g (12.9 mmol) of the donor (*o*-nitrophenyl *β*-D-[1-^{13}C]galactopyranoside). After the reaction was quenched, the mixture was concentrated *in vacuo* at 313 K to ∼45 ml and applied to a column (2.5 × 55 cm) of Sepharose G10. Elution with distilled water gave a phenol–sulfuric acid (Hodge & Hofreiter, 1962) positive peak near the column void volume. This disaccharide-containing fraction was collected, concentrated to ∼35 ml, and the solution was applied to a column (2.5 × 55 cm) of Dowex 1 × 2 (200–400 mesh) (OH^-) ion-exchange resin (Austin *et al.*, 1963). Elution with distilled water (3.8 ml fraction^{-1}, 0.8 ml min^{-1}) gave three phenol–sulfuric acid positive peaks. NMR analysis of each peak indicated the following: peak 1, residual acceptor; peak 2, (II); peak 3, methyl *β*-D-[1-^{13}C]galactopyranosyl-(1→3)-*β*-D-glucopyranoside (by-product). Fractions containing (II) were pooled and the volume reduced to give a clear colorless viscous syrup for characterization by ^{1}H and ^{13}C NMR.

Crystals of (II) suitable for X-ray diffraction were grown using a λ tube (Gravatt & Gross, 1969) and a modification of published protocols (Hope, 1971). Approximately 20 mg of (II) were dissolved in 300 ml of distilled water and the solution was placed in the sample reservoir of a λ tube. A Nichrome wire was wrapped around the arm closer to the sample reservoir for heating purposes, and a length of copper wire was closely wound around the cross arm to act as cooling ribs. The apparatus was gently filled with a 1:3:6 (*v*/*v*/*v*) mixture of *n*-butanol–methanol–ethanol to a level above the cross arm, the open ends were stoppered, and a low electric current was applied across the Nichrome wire to heat the ascending arm to ∼323 K. After 10 d, a tiny needle-shaped crystal formed in the cooler descending arm of the λ tube. This crystal was carefully removed, placed in a capped vial with mother liquor that had been significantly reduced in volume, and the vessel was set at room temperature. The vial was not tightly capped so as to allow slow evaporation of solvent. After about 18 months, colorless needle-shaped crystals formed, which were harvested for structure determination.

Crystallographic data were collected through the SCrALS (Service Crystallography at Advanced Light Source) program at the Small-Crystal Crystallography Beamline 11.3.1 (developed by the Experimental Systems Group) at the Advanced Light Source (ALS).

Crystal data

$C_{13}H_{24}O_{11}\cdot H_2O$	V = 822.6 (8) Å^3
M_r = 374.34	Z = 2
Monoclinic, $P2_1$	Synchrotron radiation
a = 7.528 (2) Å	λ = 0.77490 Å
b = 8.744 (4) Å	μ = 0.14 mm^{-1}
c = 12.695 (11) Å	T = 150 K
β = 100.15 (4)°	0.12 × 0.06 × 0.01 mm

Table 1
Structural parameters (Å, °) for (II), (II$_C$), (III) and (IV).

Bond distance standard uncertainties for (III) were not provided in the original article but were stated as being in the range 0.002–0.003 Å.

	(II)	(II$_C$)	(III)	(IV)
C1—C2	1.525 (4)	1.529	1.521	1.516 (3)
C2—C3	1.532 (4)	1.524	1.515	1.519 (3)
C3—C4	1.540 (4)	1.527	1.514	1.531 (3)
C4—C5	1.521 (4)	1.538	1.528	1.530 (3)
C5—C6	1.515 (4)	1.523	1.510	1.508 (3)
C1′—C2′	1.528 (4)	1.533	1.515	1.527 (3)
C2′—C3′	1.526 (4)	1.524	1.526	1.531 (3)
C3′—C4′	1.536 (4)	1.545	1.521	1.521 (3)
C4′—C5′	1.523 (4)	1.533	1.533	1.521 (3)
C5′—C6′	1.510 (4)	1.527	1.514	1.511 (3)
C1—O1	1.397 (4)	1.388	1.393	1.384 (3)
C1—O5	1.408 (3)	1.425	1.428	1.413 (3)
C2—O2	1.439 (4)	1.420	1.420	1.418 (3)
C3—O3	1.432 (3)	1.422	1.433	1.421 (3)
C4—O4	1.419 (3)	1.418	1.438	
C5—O5	1.427 (3)	1.429	1.430	1.428 (3)
C6—O6				1.424 (3)
C1′—O1′	1.400 (3)	1.397	1.390	1.387 (3)
C1′—O5′	1.426 (3)	1.418	1.415	1.425 (3)
C2′—O2′	1.422 (4)	1.419	1.427	1.414 (3)
C3′—O3′	1.413 (3)	1.433	1.422	1.422 (3)
C4′—O4′	1.434 (4)	1.415	1.433	1.423 (3)
C5′—O5′	1.442 (3)	1.432	1.424	1.432 (3)
C6′—O6′	1.437 (4)	1.418	1.426	1.426 (3)
C4—O1′				1.437 (3)
C6—O1′	1.441 (3)	1.430	1.425	
C1′—O1′—C4				116.2 (2)
C1′—O1′—C6	114.2 (2)	115.4	113.3	
C1—O1—C7	112.3 (2)	114.3		113.7 (2)
C2—C1—O1—C7 (*φ*)	177.4 (3)	167.4		164.2 (2)
C2′—C1′—O1′—C6 (*φ′*)	172.9 (2)	160.8	−176.4	
C2′—C1′—O1′—C4 (*φ′*)				153.8 (2)
C1′—O1′—C6—C5 (*ψ′*)	−117.9 (3)	−104.6	−156.3	
C1′—O1′—C4—C5 (*ψ′*)				−161.3 (2)
O5—C5—C6—O1′ (*ω*)	63.8 (3) (*gt*)	61.8 (*gt*)	−61.6 (*gg*)	
O5—C5—C6—O6 (*ω*)				−54.6 (2) (*gg*)
C4—C5—C6—O1′ (*ω*)	−176.2 (2)	−177.5	59.5	
C4—C5—C6—O6 (*ω*)				66.4
O5′—C5′—C6′—O6′ (*ω′*)	59.5 (3) (*gt*)	59.5 (*gt*)	−53.7 (*gg*)	57.3 (2) (*gt*)
C4′—C5′—C6′—O6′ (*ω′*)	179.9 (2)	−177.9	66.1	177.8

Notes: *gt* is *gauche–trans*; *gg* is *gauche–gauche*.

Table 2
Cremer–Pople pyranosyl ring-puckering parameters for (II), (II_C), (III), ($I_{G1–G3}$) and (IV).

	q_2	q_3	Q	φ (°)	θ (°)
βGal*p* ring†					
II	0.0877	0.5700	0.5767	312.8	8.8
II_C	0.0620	0.5545	0.5580	39.8	6.4
III	0.0481	0.5491	0.5512	33.3	5.0
I_{G1}	0.0414	0.5730	0.5745	18.2	4.1
I_{G2}	0.0356	0.5850	0.5861	353.6	3.5
I_{G3}	0.0159	0.5532	0.5534	28.0	1.7
IV	0.0485	0.5928	0.5948	28.2	4.7
βGlc*p* ring					
II	0.0237	0.5999	0.6004	6.4	2.3
II_C	0.0279	0.5785	0.5791	37.2	2.8
III	0.0756	0.5763	0.5812	22.3	7.5
I_{G1}	0.2363	0.5088	0.5610	19.5	24.9
I_{G2}	0.3039	0.4793	0.5675	347.5	32.4
I_{G3}	0.1737	0.5589	0.5852	159.1	17.3
IV	0.1159	0.5475	0.5579	341.5	12.0

† In (III), the βGal*p* ring is replaced by a βGlc*p* ring.

Data collection

Bruker D8 APEXII CCD diffractometer
Absorption correction: multi-scan (*SADABS*; Sheldrick, 2007)
T_{min} = 0.984, T_{max} = 0.999
10449 measured reflections
2192 independent reflections
1920 reflections with $I > 2\sigma(I)$
R_{int} = 0.087

Refinement

$R[F^2 > 2\sigma(F^2)]$ = 0.049
$wR(F^2)$ = 0.121
S = 1.05
2192 reflections
239 parameters
3 restraints
H atoms treated by a mixture of independent and constrained refinement
$\Delta\rho_{max}$ = 0.41 e Å^{-3}
$\Delta\rho_{min}$ = −0.39 e Å^{-3}

All H atoms were located from a difference Fourier map. Carbon-bound and hydroxy H atoms were subsequently treated as riding atoms in geometrically idealized positions, with C—H distances of 1.00 (methine), 0.99 (methylene) or 0.98 Å (methyl) and O—H distances of 0.84 Å. The H atoms on the water of crystallization were restrained to have O—H distances of 0.84 (2) Å. For all H atoms, U_{iso}(H) = kU_{eq}(carrier), where k = 1.5 for the methyl groups, which were permitted to rotate but not to tilt, and k = 1.2 for all other H atoms.

The assignment of the correct absolute configuration of the molecule and enantiomorph of the space group were determined by comparison with the same compound that had been previously characterized with Cu $K\alpha$ radiation. That previous analysis had determined the correct configuration by comparison of intensities of Friedel pairs of reflections and by the known configuration of the allolactoside.

Data collection: *APEX2* (Bruker, 2007); cell refinement: *APEX2* and *SAINT* (Bruker, 2007); data reduction: *SAINT* and *XPREP* (Sheldrick, 2008); program(s) used to solve structure: *SHELXS97* (Sheldrick, 2008); program(s) used to refine structure: *SHELXL97* (Sheldrick, 2008); molecular graphics: *XP* (Sheldrick, 2008), *POV-RAY* (Cason, 2003) and *DIAMOND* (Brandenburg, 2009); software used to prepare material for publication: *XCIF* (Sheldrick, 2008), *enCIFer* (CCDC, 2005) and *publCIF* (Westrip, 2009).

The sample was submitted for crystallographic analysis through the SCrALS (Service Crystallography at Advanced Light Source) program. Crystallographic data were collected at Beamline 11.3.1 at the Advanced Light Source (ALS), Lawrence Berkeley National Laboratory. The ALS is supported by the US Department of Energy, Office of Energy Sciences, Materials Sciences Division, under contract No. DE-AC02-05CH11231 at Lawrence Berkeley National Laboratory.

Table 3
Structural parameters (°) for ($I_{G1–G3}$).

	(I_{G1})	(I_{G2})	(I_{G3})
C1′—O1′—C6	111.9	114.3	109.0
C2′—C1′—O1′—C6 (φ')	174.0	170.0	171.0
C1′—O1′—C6—C5 (ψ')	−158.4	−168.3	−162.4
O5—C5—C6—O1′ (ω)	69.4 (*gt*)	66.0 (*gt*)	−86.8 (*gg*)
C4—C5—C6- O1′ (ω)	−169.7	−176.0	32.7
O5′—C5′—C6′—O6′ (ω')	−179.7 (*tg*)	−171.6 (*tg*)	−179.7 (*tg*)
C4′—C5′—C6′—O6′ (ω')	−56.3	−50.8	−57.7

Notes: *gt* is *gauche–trans*; *gg* is *gauche–gauche*; *tg* is *trans–gauche*.

Table 4
Hydrogen-bond geometry (Å, °).

D—H···A	D—H	H···A	D···A	D—H···A
O2—H2···O2′^{i}	0.84	2.38	3.089 (3)	142
O2—H2···O3′^{i}	0.84	2.58	3.280 (3)	141
O3—H3···O4′^{ii}	0.84	1.90	2.695 (3)	157
O4—H4···O1W^{iii}	0.84	2.03	2.828 (3)	157
O2′—H2′···O1^{iv}	0.84	1.90	2.693 (3)	156
O3′—H3′···O3^{v}	0.84	1.99	2.796 (4)	162
O4′—H4′···O1W^{vi}	0.84	1.87	2.698 (4)	169
O6′—H6′···O2′^{vii}	0.84	1.95	2.781 (3)	170
O1W—H1WA···O2^{i}	0.829 (19)	1.93 (2)	2.750 (3)	168 (4)
O1W—H1WB···O6′^{viii}	0.840 (19)	1.89 (2)	2.724 (3)	170 (4)

Symmetry codes: (i) $-x+2, y+\frac{1}{2}, -z+1$; (ii) $-x+1, y+\frac{1}{2}, -z+1$; (iii) $-x+1, y-\frac{1}{2}, -z+1$; (iv) $-x+2, y-\frac{1}{2}, -z+1$; (v) $x, y, z-1$; (vi) $-x+1, y-\frac{1}{2}, -z$; (vii) $x-1, y, z$; (viii) $x+1, y, z$.

Supplementary data for this paper are available from the IUCr electronic archives (Reference: MX3023). Services for accessing these data are described at the back of the journal.

References

Altona, C. & Sundaralingam, M. (1972). *J. Am. Chem. Soc.* **94**, 8205–8212.
Altona, C. & Sundaralingam, M. (1973). *J. Am. Chem. Soc.* **95**, 2333–2344.
Angyal, S. J., Bethell, G. S. & Beveridge, R. (1979). *Carbohydr. Res.* **73**, 9–18.
Arène, F., Neuman, A. & Longchambon, F. (1979). *C. R. Acad. Sci. Paris Ser.* **288**, 331–334.
Austin, P. W., Hardy, F. E., Buchanan, J. C. & Baddiley, J. (1963). *J. Chem. Soc.* pp. 5350–5353.
Becke, A. D. (1993). *J. Chem. Phys.* **98**, 5648–5652.
Berman, H. M., Chu, S. C. & Jeffery, G. A. (1967). *Science*, **157**, 1576–1577.
Brandenburg, K. (2009). *DIAMOND*. Crystal Impact GbR, Bonn, Germany.
Bruker (2007). *APEX2* and *SAINT*. Bruker AXS Inc., Madison, Wisconsin, USA.
Burstein, C., Cohn, M., Kepes, A. & Monod, J. (1965). *Biochim. Biophys. Acta*, **95**, 634–639.
Cason, C. J. (2003). *POV-RAY*. Persistence of Vision Raytracer Pty Ltd, Victoria, Australia.
CCDC (2005). *enCIFer*. Cambridge Crystallographic Data Centre, 12 Union Road, Cambridge, England.
Conchie, J. & Levvy, G. A. (1963). *Methods Carbohydr. Chem.* **2**, 335–337.
Cremer, D. & Pople, J. A. (1975). *J. Am. Chem. Soc.* **97**, 1354–1358.
Foloppe, N. & Nilsson, L. (2005). *J. Phys. Chem. B*, **109**, 9119–9131.
French, A. D. & Finch, P. (1999). *Carbohydrates: Structures, Syntheses and Dynamics*, edited by P. Finch, pp. 1–46. Boston: Kluwer Academic Publishers.

Frisch, M. J., *et al.* (2004). *GAUSSIAN03*. Revision C.02. Gaussian Inc., Wallingford, CT, USA.
Gravatt, C. C. & Gross, P. M. (1969). *J. Chem. Educ.* **46**, 693–694.
Hehre, W. J., Ditchfield, R. & Pople, J. A. (1972). *J. Chem. Phys.* **56**, 2257–2261.
Hodge, J. E. & Hofreiter, B. T. (1962). *Methods Carbohydr. Chem.* **1**, 380–394.
Hope, H. (1971). *J. Appl. Cryst.* **4**, 333.
Jacob, F. & Monod, J. (1961). *J. Mol. Biol.* **3**, 318–356.
Jeffrey, G. A. & Yates, J. H. (1979). *Carbohydr. Res.* **74**, 319–322.
Jobe, A. & Bourgeois, S. (1972). *J. Mol. Biol.* **69**, 397–408.
Juers, D. H., Heightman, T. D., Vasella, A., McCarter, J. D., Mackenzie, L., Withers, S. G. & Matthews, B. W. (2001). *Biochemistry*, **40**, 14781–14794.
Kubo, H., Jiang, G. J., Irie, A., Morita, M., Matsubara, T. & Hoshi, M. (1992). *J. Biochem.* **111**, 726–731.
Lemieux, R. U. (1971). *Pure Appl. Chem.* **25**, 527–548.
Mir, R., Singh, N., Sinha, M., Sharma, S., Bhushan, A. & Singh, T. P. (2009). In preparation.
Nilsson, K. G. I. (1987). *Carbohydr. Res.* **167**, 95–103.
Nilsson, K. G. I. (1988). *Carbohydr. Res.* **180**, 53–59.
Pan, Q., Noll, B. C. & Serianni, A. S. (2005). *Acta Cryst.* C**61**, o674–o677.
Rohrer, D. C., Sarko, A., Bluhm, T. L. & Lee, Y. N. (1980). *Acta Cryst.* B**36**, 650–654.
Serianni, A. S., Nunez, H. A. & Barker, R. (1979). *Carbohydr. Res.* **72**, 71–78.
Serianni, A. S., Vuorinen, T. & Bondo, P. B. (1990). *J. Carbohydr. Chem.* **9**, 513–541.
Sheldrick, G. M. (2007). *SADABS*. University of Göttingen, Germany.
Sheldrick, G. M. (2008). *Acta Cryst.* A**64**, 112–122.
Stenutz, R., Shang, M. & Serianni, A. S. (1999). *Acta Cryst.* C**55**, 1719–1721.
Thibaudeau, T., Stenutz, R., Hertz, B., Klepach, T. E., Zhao, S., Wu, Q., Carmichael, I. & Serianni, A. S. (2004). *J. Am. Chem. Soc.* **126**, 15668–15685.
Westrip, S. P. (2009). *publCIF*. In preparation.
Yildirim, N. & Mackey, M. C. (2003). *Biophys. J.* **84**, 2841–2851.